Science Advances
AAAS

Supplementary Materials for

Release of CHK-2 from PPM-1.D anchorage schedules meiotic entry

Antoine Baudrimont, Dimitra Paouneskou, Ariz Mohammad, Raffael Lichtenberger, Joshua Blundon, Yumi Kim, Markus Hartl, Sebastian Falk, Tim Schedl, Verena Jantsch*

*Corresponding author. Email: verena.jantsch@univie.ac.at

Published 16 February 2022, *Sci. Adv.* **8**, eabl8861 (2022)
DOI: 10.1126/sciadv.abl8861

The PDF file includes:

Figs. S1 to S14
Tables S1, S4 to S15
Legends for tables S2 and S3
References

Other Supplementary Material for this manuscript includes the following:

Tables S2 and S3

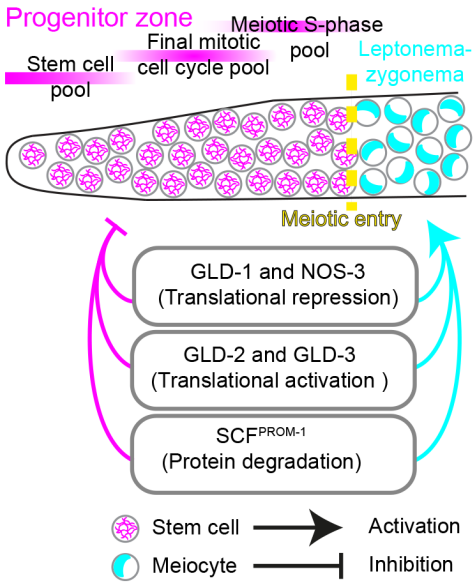

Fig. S1.

Control of progenitor cell fate and meiotic entry in *C. elegans*. Schematic diagram of the distal part of the *C. elegans* gonad, with the progenitor zone shown in magenta; it consists of three different pools of cells (stem cell pool, final mitotic cell cycle pool, meiotic S-phase pool). Cells in leptonema–zygonema are half-moon shaped (cyan). The lower part delineates the three genetic pathways involved in the control of the germline stem cell fate versus meiosis/differentiation.

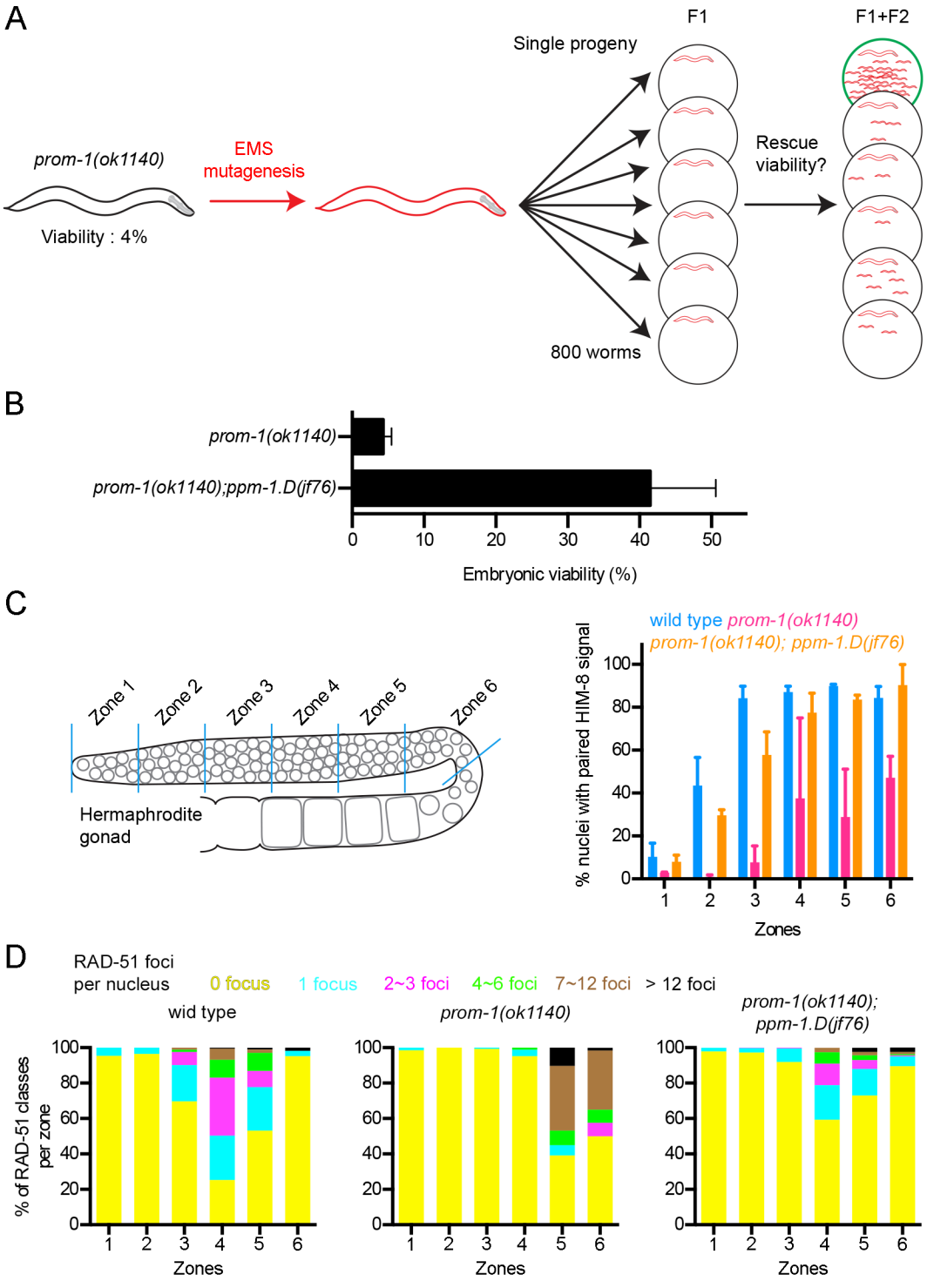

Fig. S2.

Identification of *prom-1* suppressor and characterization of the double mutant *prom-1(ok1140); ppm-1.D(jf76)*. (A) Schematic diagram of the suppressor screen. Single F1

heterozygotes were screened after mutagenesis and suppressor candidate scores were based on the viability/population density on the individual plates. (B) Viability of *prom-1(ok1140)* and the suppressor line *prom-1(ok1140); ppm-1.D(jf76)*. (C) Left, *C. elegans* hermaphrodite gonad divided into six zones of equal length. Right, percentage pairing of X chromosomes (scored with HIM-8) in the different zones for the indicated genotypes. (D) Quantification of RAD-51 foci in the different zones of the indicated genotypes.

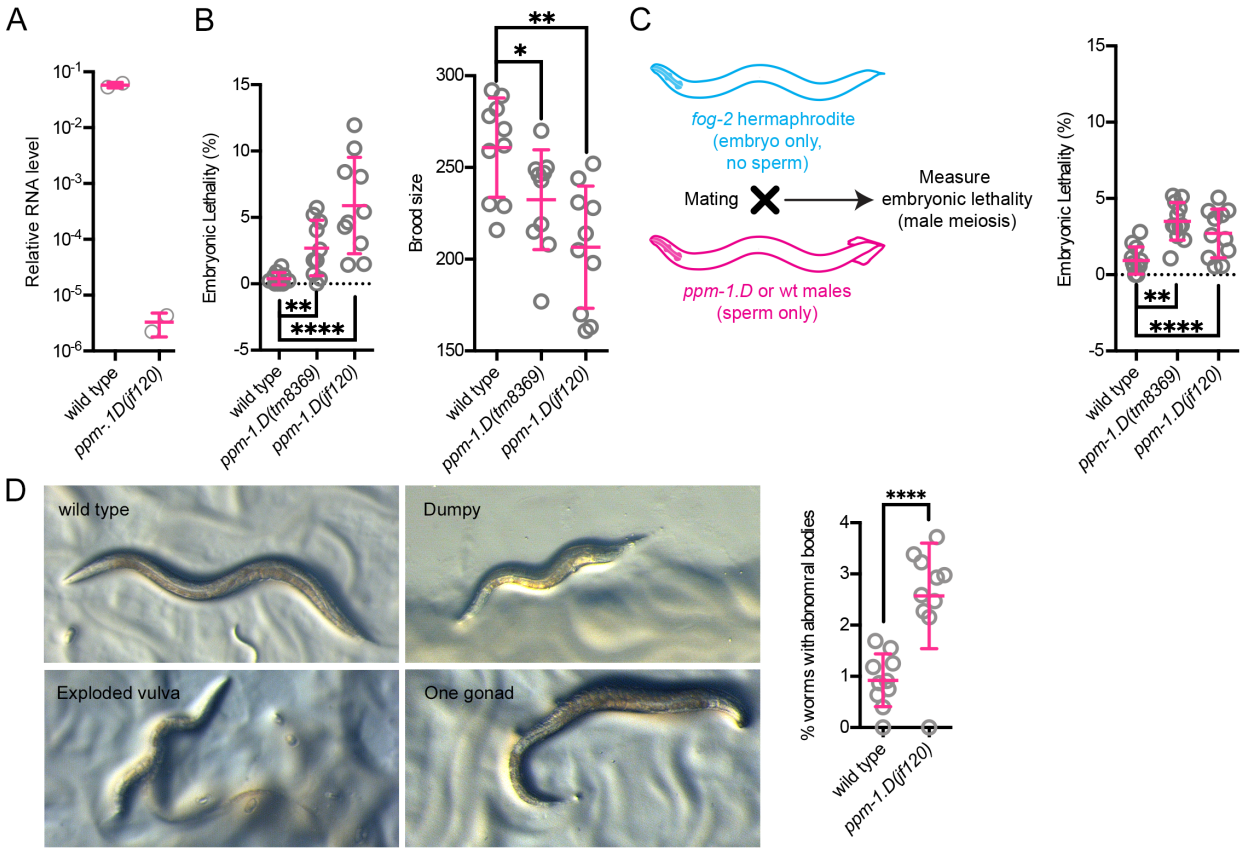

Fig. S3.

***ppm-1.D* mutants have low levels of unhatched embryos originating from defects in both oogenesis and spermatogenesis.** (A) Relative levels of *ppm-1.D* RNA in the indicated genotypes. (B) Left, percentage embryonic lethality for the indicated genotypes. Right, brood size counts for the indicated genotypes. (C) Left, *ppm-1.D* mutant males were mated to *fog-2* mutants to assay male meiosis. Right, percentage of non-hatching eggs for the indicated genotypes. **P* < 0.05, ***P* < 0.01, *****P* < 0.0001 for the Mann–Whitney test. (D) Left, representative pictures of abnormal body morphologies observed in *ppm-1.D(jf120)*. Right, quantification of abnormal body morphologies in wild-type and *ppm-1.D(jf120)* worms. In all, 2,000 synchronized worms were screened for abnormal body morphologies for each genotype. *****P* < 0.0001 for the Chi-square test.

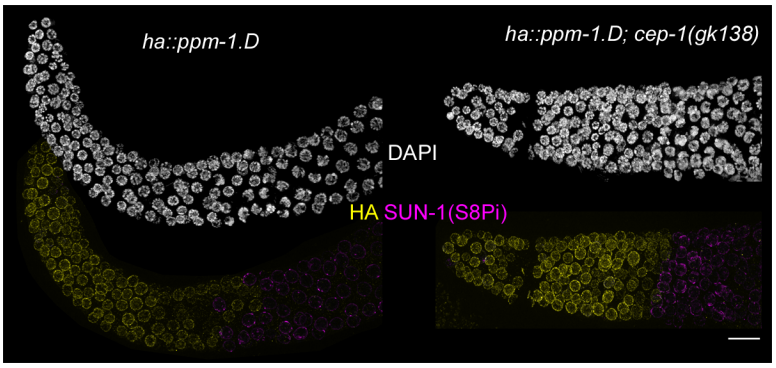

Fig. S4.

PPM-1.D expression in the progenitor zone is not controlled by *cep-1*. DAPI staining and immunostaining for HA::PPM-1.D (yellow) and SUN-1(S8Pi) (magenta) for the indicated genotypes. Scale bar: 10 µm

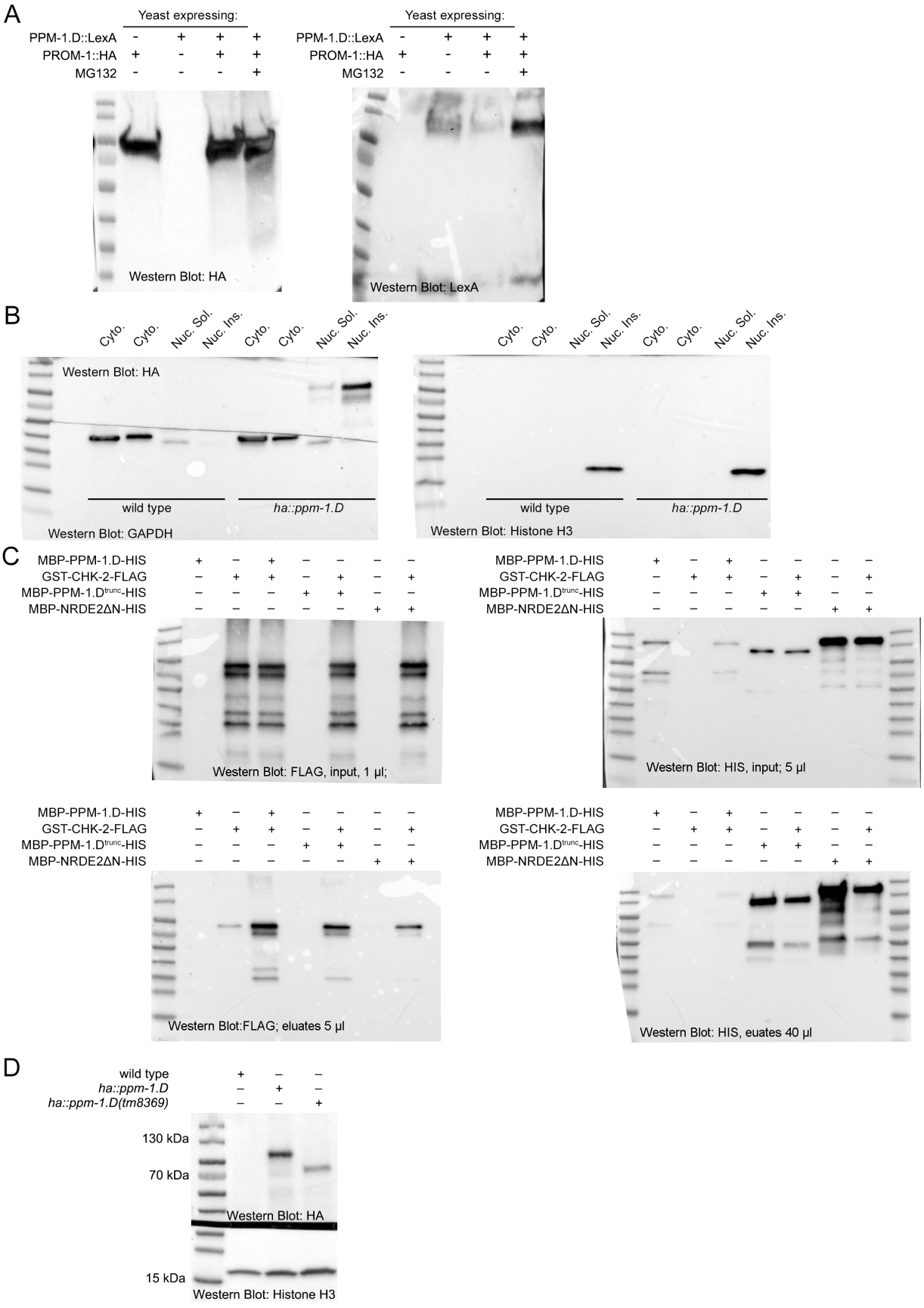
A
Yeast expressing:
PPM-1.D::LexA - + + +
PROM-1::HA + - + +
MG132 - - - +
Western Blot: HA
Yeast expressing:
PPM-1.D::LexA - + + +
PROM-1::HA + - + +
MG132 - - - +
Western Blot: LexA
B
Cyto. Cyto. Nuc. Sol. Nuc. Ins. Cyto. Cyto. Nuc. Sol. Nuc. Ins.
Western Blot: HA
wild type
ha::ppm-1.D
Western Blot: GAPDH
Cyto. Cyto. Nuc. Sol. Nuc. Ins. Cyto. Cyto. Nuc. Sol. Nuc. Ins.
wild type
ha::ppm-1.D
Western Blot: Histone H3
C
MBP-PPM-1.D-HIS + – + – – – –
GST-CHK-2-FLAG – + + – + – +
MBP-PPM-1.D^trunc-HIS – – – + + – –
MBP-NRDE2ΔN-HIS – – – – – + +
Western Blot: FLAG, input, 1 µl;
MBP-PPM-1.D-HIS + – + – – – –
GST-CHK-2-FLAG – + + – + – +
MBP-PPM-1.D^trunc-HIS – – – + + – –
MBP-NRDE2ΔN-HIS – – – – – + +
Western Blot: HIS, input; 5 µl
MBP-PPM-1.D-HIS + – + – – – –
GST-CHK-2-FLAG – + + – + – +
MBP-PPM-1.D^trunc-HIS – – – + + – –
MBP-NRDE2ΔN-HIS – – – – – + +
Western Blot:FLAG; eluates 5 µl
MBP-PPM-1.D-HIS + – + – – – –
GST-CHK-2-FLAG – + + – + – +
MBP-PPM-1.D^trunc-HIS – – – + + – –
MBP-NRDE2ΔN-HIS – – – – – + +
Western Blot: HIS, euates 40 µl
D
wild type + – –
ha::ppm-1.D – + –
ha::ppm-1.D(tm8369) – – +
130 kDa
70 kDa
Western Blot: HA
15 kDa
Western Blot: Histone H3

Fig. S5.

Full photographs of the western blots shown in Figs. 2, 3 and 4. (A) Western blot analysis of TCA-precipitated proteins from yeast expressing PPM-1.D::LexA or PROM-1::HA in the absence or presence of the proteasome inhibitor MG132. (B) Western blot analysis of cellular fractions (cytosolic, soluble nuclear and insoluble nuclear) using the specified antibodies for the indicated genotypes. (C) Western blot analysis after amylose purification of the indicated proteins expressed in *E. coli*. (D) Western blot analysis of HA and histone H3 in whole worm extracts, for the indicated genotypes.

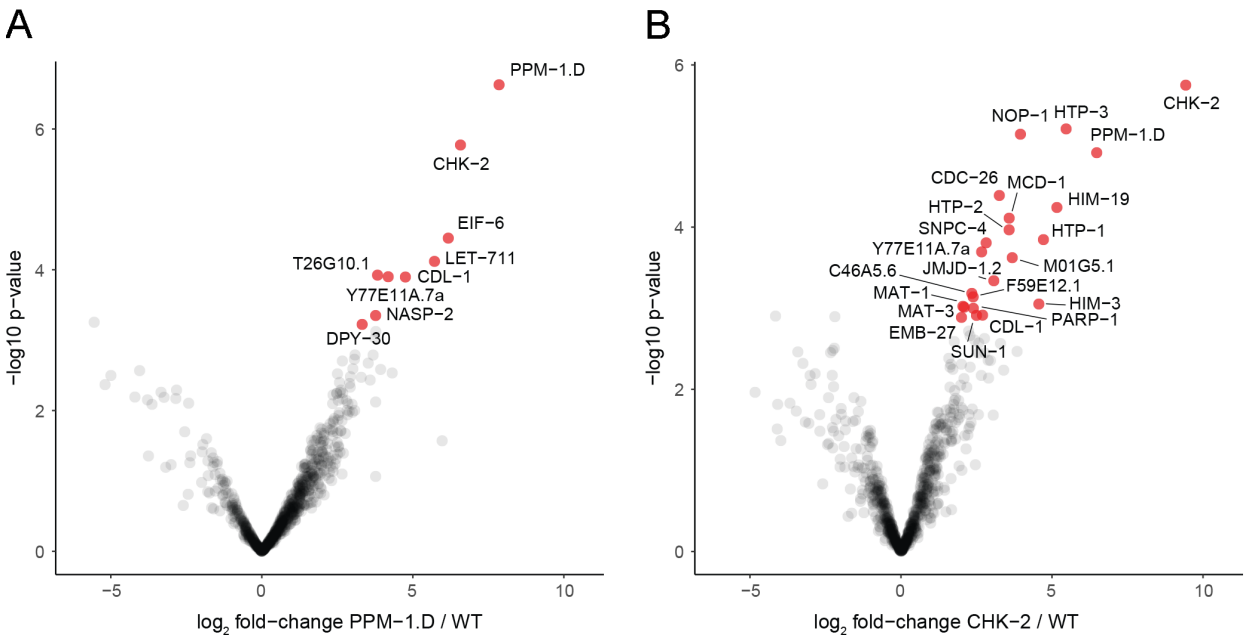

Fig. S6.

Volcano plots of mass spectrometry data for HA::PPM-1.D and CHK-2::HA, triplicate experiments. Interacting proteins for PPM-1.D (A) and CHK-2 (B) bait proteins compared with the wild-type control, as determined by affinity-enrichment mass spectrometry. LIMMA was used for statistical analysis. Proteins marked in red were considered to be enriched at an adjusted *P* value of < 0.05 and a fold-change of > 2.

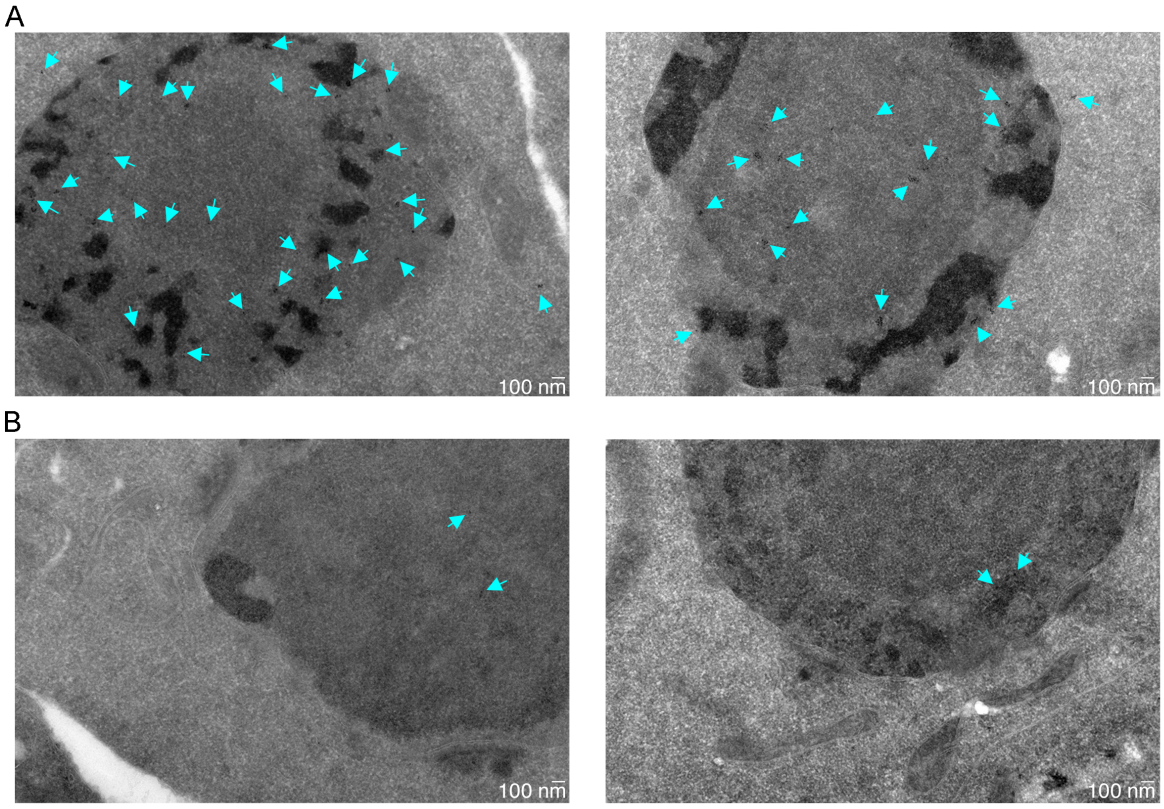

Fig. S7.

Specificity of the antibody used for electron microscopy localization of CHK-2. (A) Representative pictures of mitotic nuclei at 14,000× resolution, with cyan arrows highlighting the gold particles linked to the secondary antibody recognizing the bound anti-CHK-2 antibody. (B) Representative pictures of mitotic nuclei at 14,000× resolution with cyan arrows highlighting the gold particles linked to the secondary antibody with no primary antibody.

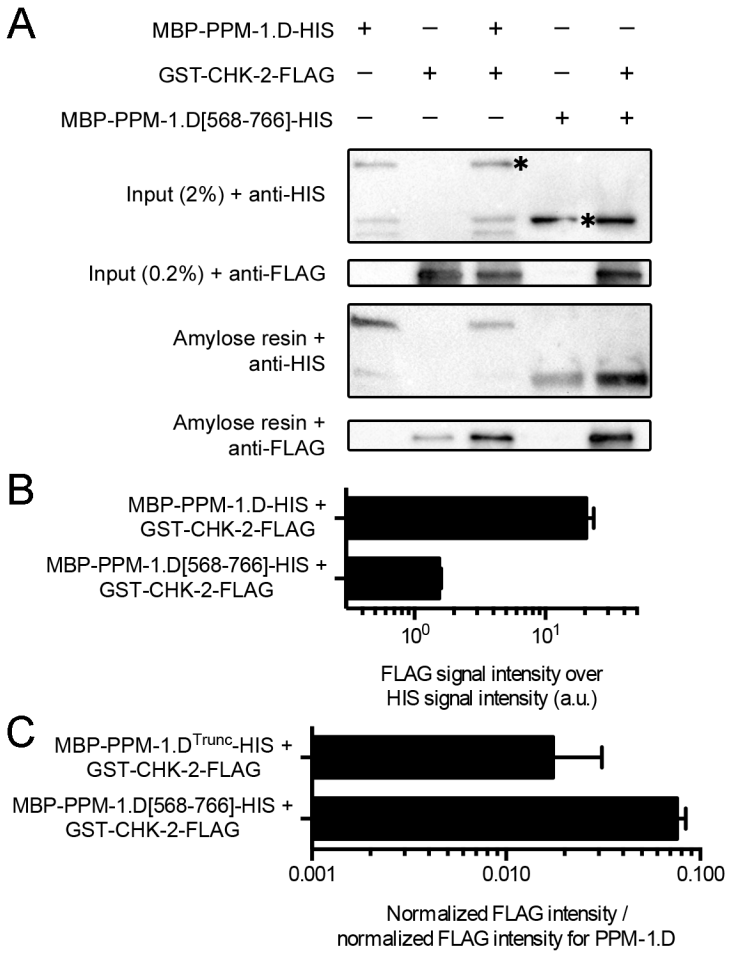

Fig. S8.

The C-terminal region of PPM-1.D binds to CHK-2. (A) Western blot analysis after amylose pull down experiments of the indicated proteins expressed in *E. coli*. Asterisks mark the corresponding bands on the blot. (B) Quantification of the FLAG signal (CHK-2) normalized to the HIS signal for the indicated co-lysed samples. (C) Ratio of the normalized FLAG intensity for PPM-1.D^{trunc} or PPM-1.D[568-766] to the normalized FLAG intensity for full-length PPM-1.D. Normalization was to HIS signal intensity in both cases. (n = 2 biological replicates).

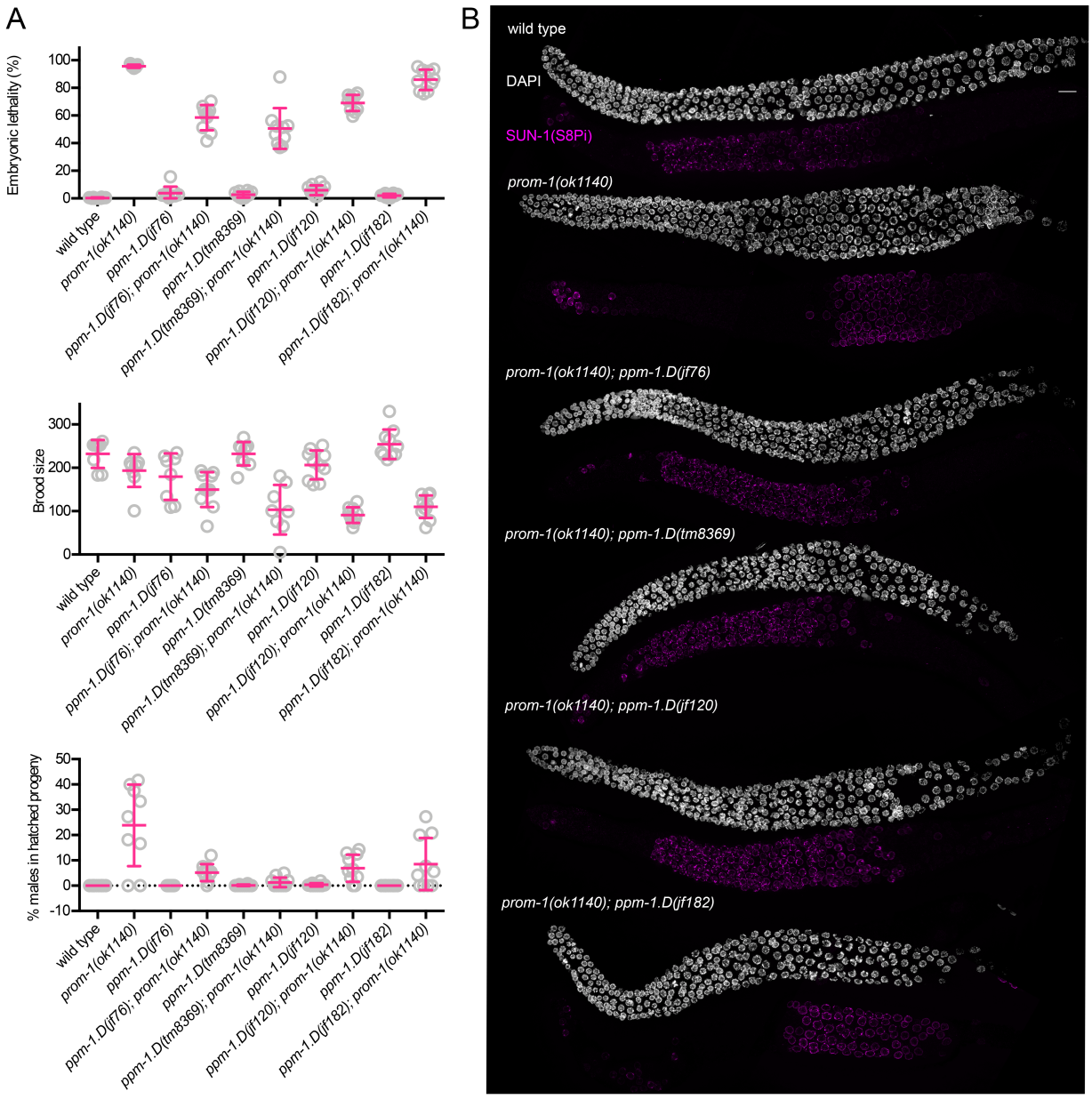
A
Embryonic lethality (%)
100
80
60
40
20
0
wild type
prom-1(ok1140)
ppm-1.D(jf76)
ppm-1.D(jf76); prom-1(ok1140)
ppm-1.D(tm8369)
ppm-1.D(tm8369); prom-1(ok1140)
ppm-1.D(jf120)
ppm-1.D(jf120); prom-1(ok1140)
ppm-1.D(jf182)
ppm-1.D(jf182); prom-1(ok1140)
Brood size
300
200
100
0
% males in hatched progeny
50
40
30
20
10
0
-10
B
wild type
DAPI
SUN-1(S8Pi)
prom-1(ok1140)
prom-1(ok1140); ppm-1.D(jf76)
prom-1(ok1140); ppm-1.D(tm8369)
prom-1(ok1140); ppm-1.D(jf120)
prom-1(ok1140); ppm-1.D(jf182)
C
Number DAPI bodies at -1 diakinesis
12
10
8
6
4
2
0

Fig. S9.

Suppression of the *prom-1* phenotype by different alleles of *ppm-1.D*. (A) Embryonic lethality (top), brood size (middle) and percentage of males in the progeny (bottom) for the indicated genotypes; Alleles of *ppm-1.D* are *jf76* (suppressor allele identified in the screen—with a point mutation leading to protein truncation), *tm8369* (truncation), *jf120* (full deletion of *ppm-1.D*), and *jf182* (PPM-1.D is catalytically dead). Diagonal matrices of *P* values from Mann–Whitney tests comparing the different genotypes are shown in table S12 (embryonic lethality), table S13 (brood size), and table S14 (percentage of males). (B) DAPI staining and SUN-1(S8Pi) immunostaining (magenta) for the indicated genotypes. Scale bar: 10 μm. (C) Number of DAPI bodies at -1 diakinesis for the indicated genotypes. A diagonal matrix for *P* values from Mann–Whitney tests comparing the different genotypes is shown in table S15.

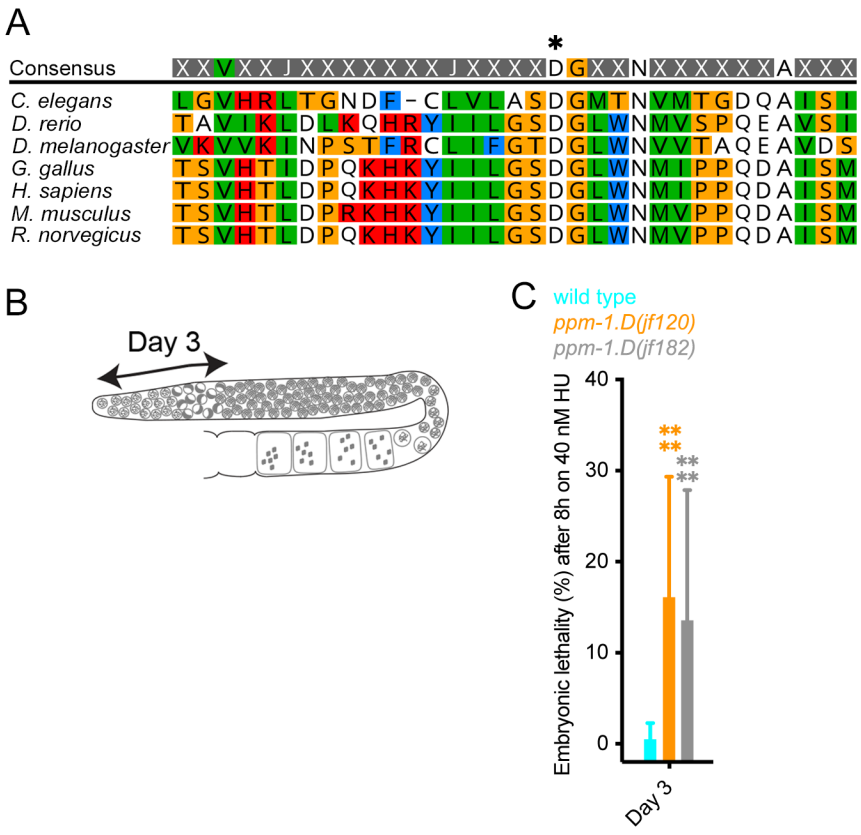

Fig. S10.

Validation of catalytically inactive PPM-1.D. (A) Alignment of PPM-1.D protein sequences (amino acids 498–530) for the indicated organisms, highlighting conservation of the PP2C domain. The asterisk marks the conserved aspartic acid required for the phosphatase activity) (B) Schematic diagram of the *C. elegans* germline indicating the position of nuclei in the gonad at the time of the HU treatment and the day at which embryonic viability can be measured. (C) Embryonic lethality at 3 days after an 8 h treatment with on 40 nM HU for the indicated genotypes. *jf120* allele is a null allele of *ppm-1.D* and *jf182* encodes catalytically inactive PPM-1.D. ****$P < 0.0001$ for the Student's T-test.

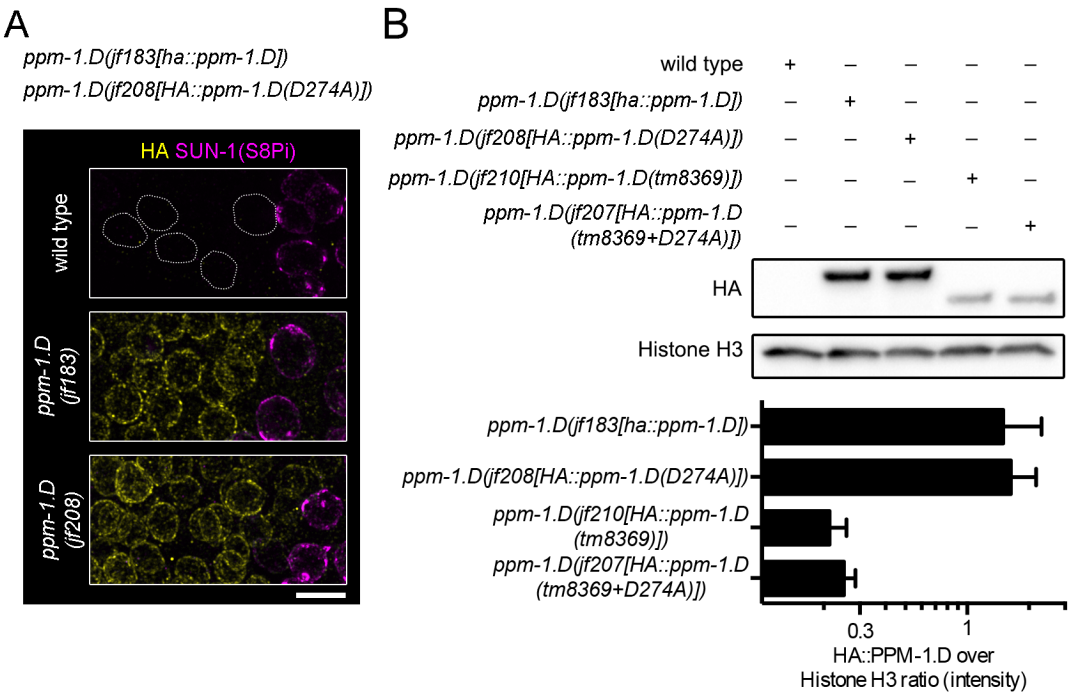

Fig. S11.

Subcellular localization and protein stability are unaffected in catalytically inactive PPM-1.D. (A) Immunostaining for HA::PPM-1.D (yellow) and SUN-1(S8Pi) (magenta) for the indicated genotypes. Scale bar: 5 µm. (B) Top, western blot analysis of whole worm extracts for HA::PPM-1.D and histone H3. Bottom, quantification of the ratio of HA::PPM-1.D to histone H3 for the indicated genotypes. (n = 2 western blots).

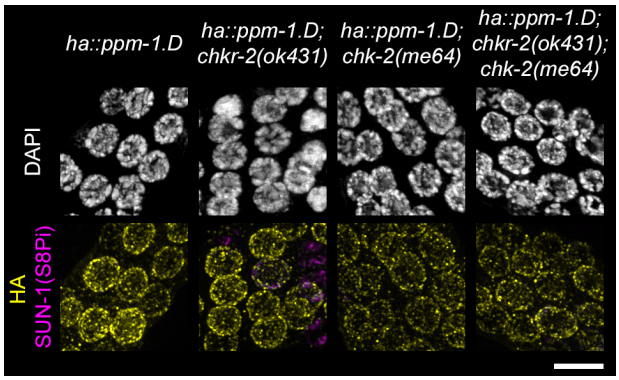

Fig. S12.

HA::PPM-1.D localization at the nuclear periphery is independent of *chk-2* and its paralog *chkr-2*. DAPI staining and immunostaining of HA (yellow) and SUN-1(S8Pi) (magenta) for the indicated genotypes. Scale bar: 5 μm

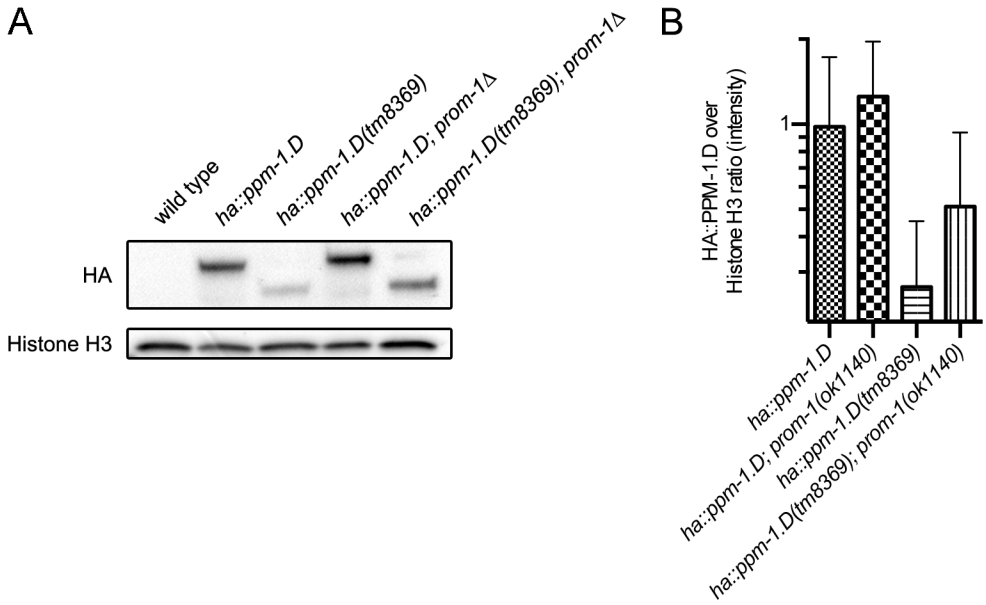

Fig. S13.

PPM-1.D^{trunc} is regulated by the SCF^{PROM-1} complex. (A) Western blot analysis of whole worm extracts for HA::PPM-1.D and histone H3. (B) Quantification of the ratio of HA::PPM-1.D to histone H3 for the indicated genotypes (n = 3 western blots). Data for the wild-type, *ha::ppm-1.D* and *ha::ppm-1.D(tm8369)* are the same in (A) and (B) as in Fig. 4C.

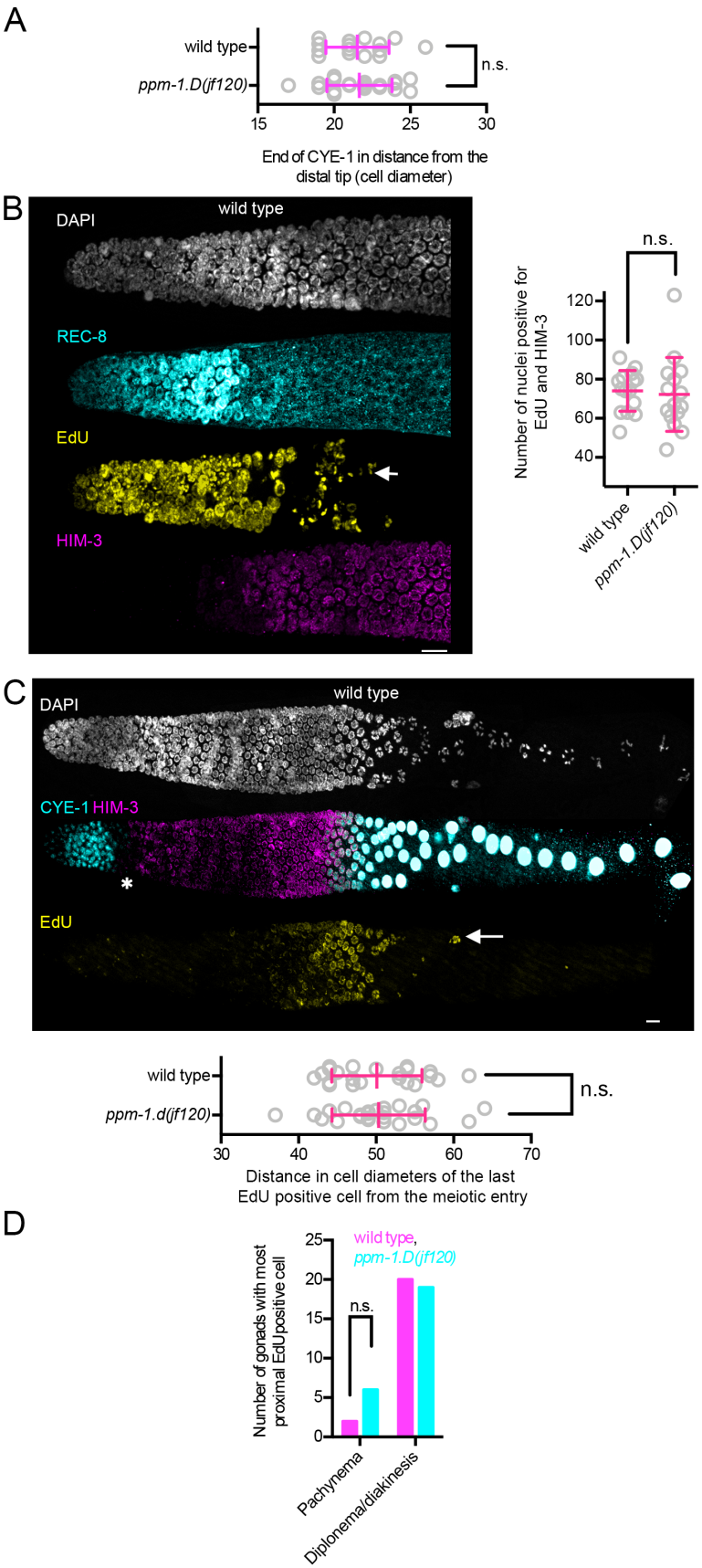
A
wild type
ppm-1.D(jf120)
n.s.
15
20
25
30
End of CYE-1 in distance from the distal tip (cell diameter)
B
DAPI
wild type
REC-8
EdU
HIM-3
n.s.
Number of nuclei positive for EdU and HIM-3
120
100
80
60
40
wild type
ppm-1.D(jf120)
C
DAPI
wild type
CYE-1 HIM-3
EdU
wild type
ppm-1.d(jf120)
n.s.
30
40
50
60
70
Distance in cell diameters of the last EdU positive cell from the meiotic entry
D
wild type,
ppm-1.D(jf120)
Number of gonads with most proximal EdU positive cell
25
20
15
10
5
0
n.s.
Pachynema
Diplonema/diakinesis

Fig. S14.

The *ppm-1.D(jf120)* mutant has similar progenitor zone length, meiotic output and progression compared with the wild type. (A) Quantification of the length of the progenitor zone from the distal tip to the last cell row stained for CYE-1 (in cell diameters), for the indicated genotype. There is no significant difference (Mann–Whitney test) between wild type and *ppm-1.D(jf120)*. (B) Left, DAPI staining and immunostaining for REC-8 (cyan), EdU (yellow), and HIM-3 (magenta) in wild type at 5 hours after the EdU pulse. The arrow indicates an example nucleus that is positive for both EdU and HIM-3. Scale bar: 10 μm. Right, quantification of double EdU- and HIM-3-positive nuclei for the indicated genotypes. There is no significant difference (Mann–Whitney test) between wild type and *ppm-1.D(jf120)*. (C) Top, DAPI staining and immunostaining of CYE-1 (cyan), EdU (yellow), and HIM-3 (magenta) in wild type following a 48 h chase after the 5 h EdU pulse. The arrow indicates the most proximal EdU positive nucleus in this gonad. Scale bar: 10 μm. Bottom, quantification of the distance in cell diameters of the last EdU positive cell from meiotic entry for the indicated genotypes. There is no significant difference (Mann–Whitney test) between wild type and *ppm-1.D(jf120)*. (D) Quantification of gonads with the most proximal EdU-positive cell in pachynema or diplonema/diakinesis for the indicated genotypes at 48 h after EdU pulse. There is no significant difference (Mann–Whitney test) between wild type and *ppm-1.D(jf120)*.

Table S1.

Viability of the indicated *C. elegans* strains. The progeny of 10 worms were scored.

Strain genotype	Viability (%, mean ± SD)
Wild type	99.74 ± 0.24
prom-1::ha	99.23 ± 0.60
ha::ppm-1.D	99.66 ± 0.41
ppm-1.D::ha	96.7 ± 1.70
chk-2::ha	97.97 ± 2.28
ha::ppm-1.D; chk-2::FLAG	99.84 ± 0.25

Table S2.

Spreadsheet of all proteins identified in triplicated HA::PPM-1.D immunoprecipitation followed by mass spectrometry analysis.

Table S3.

Spreadsheet of all proteins identified in triplicate CHK-2::HA immunoprecipitation experiments followed by mass spectrometry analysis.

Table S4.

S-phase and M-phase indexes for *ppm-1.D(jf120)*

	Total nuclei	EdU positive nuclei	S-phase index	H3(S10Pi) positive nuclei	M-phase index	Number of germlines
Wild type	236 ± 18	127 ± 17	54 ± 7	6.4 ± 5	2.7 ± 2	10
ppm-1.D(jf120)	246 ± 19	135 ± 20	55 ± 6	7.8 ± 4	3.2 ± 1.5	10
z-test	$P = 0.59$		$P = 0.27$		$P = 0.16$	

Table S5.

***P* values from Fisher's Exact tests comparing the number of RAD-51 foci in the indicated mutants against wild type.** Significant values (< 0.05) are highlighted in bold.

		Number of RAD-51 foci					
Zone	Genotype	0	1	2–3	4–6	7–12	> 12
1	*ppm-1.D(tm8369)*	0.6441	> 0.9999	0.2907	> 0.9999	> 0.9999	> 0.9999
	ppm-1.D(jf120)	0.0589	0.6462	**0.0455**	0.1046	> 0.9999	> 0.9999
2	*ppm-1.D(tm8369)*	**0.0014**	0.054	**0.006**	> 0.9999	> 0.9999	> 0.9999
	ppm-1.D(jf120)	**0.0038**	**0.0155**	0.3044	> 0.9999	> 0.9999	> 0.9999
3	*ppm-1.D(tm8369)*	**0.0003**	0.3613	**0.0003**	**0.0259**	> 0.9999	> 0.9999
	ppm-1.D(jf120)	0.653	0.5834	0.6181	**0.0168**	> 0.9999	0.421
4	*ppm-1.D(tm8369)*	**0.0002**	0.0756	0.4791	**< 0.0001**	**0.0471**	0.6112
	ppm-1.D(jf120)	**< 0.0001**	**0.0006**	0.9254	**< 0.0001**	**< 0.0001**	> 0.9999
5	*ppm-1.D(tm8369)*	**< 0.0001**	0.5005	**0.0007**	**0.002**	**0.0213**	**0.0155**
	ppm-1.D(jf120)	**< 0.0001**	0.5292	**< 0.0001**	**< 0.0001**	**0.027**	> 0.9999
6	*ppm-1.D(tm8369)*	**0.0027**	**0.0181**	> 0.9999	0.1246	0.4997	0.2496
	ppm-1.D(jf120)	**< 0.0001**	**0.0011**	**0.0067**	0.0623	> 0.9999	> 0.9999

Table S6. *P* values from Mann–Whitney tests comparing the number of apoptotic corpses in the germlines of different genotypes. Significant *P* values (< 0.05) are highlighted in bold.

	Wild type	*ppm-1.D(tm8369)*	*ppm-1.D(tm8369); cep-1(gk138)*	*ppm-1.D(jf120)*	*ppm-1.D(jf120); cep-1(gk138)*	*spo-11(ok79)*	*spo-11(ok79); ppm-1.D(tm8369)*	*spo-11(ok79); ppm-1.D(jf120)*	*cep-1(gk138)*
Wild type	–	**0.0005**	0.0643	**< 0.0001**	0.9861	0.9208	**< 0.0001**	**< 0.0001**	**0.0148**
ppm-1.D(tm8369)	–	–	**< 0.0001**	**0.0004**	**0.0046**	**0.0003**	0.3133	**0.0296**	**< 0.0001**
ppm-1.D(tm8369); cep-1(gk138)	–	–	–		0.1927	**0.0401**	**< 0.0001**	**< 0.0001**	0.6193
ppm-1.D(jf120)	–	–	–	–	**< 0.0001**	**< 0.0001**	**0.0113**	0.0511	**< 0.0001**
ppm-1.D(jf120); cep-1(gk138)	–	–	–	–	–		**0.0001**	**< 0.0001**	0.1358
spo-11(ok79)	–	–	–	–	–	–	**< 0.0001**	**< 0.0001**	**0.0049**
spo-11(ok79); ppm-1.D(tm8369)	–	–	–	–	–	–	–	0.4040	**< 0.0001**
spo-11(ok79); ppm-1.D(jf120)	–	–	–	–	–	–	–	–	**< 0.0001**
cep-1(gk138)	–	–	–	–	–	–	–	–	–

Table S7.

List of *C. elegans* strains used in this study.

Strain	Source	Identifier
N2 Bristol	CGC	https://cgc.umn.edu/strain/search
prom-1(jf124[prom-1::ha])	This study	UV145
ppm-1.D(jf76)III; prom-1(ok1140) unc-55(e402) I	This study	UV157
ppm-1.D(tm8369) /qC1[dpy-19(e1259) glp-1(q339)] III	This study	UV176
ppm-1.D(tm8369) III; chk-2(jf184[chk-2::ha]) V	This study	UV177
ppm-1.D(jf120) /qC1[dpy-19(e1259) glp-1(q339)] III	This study	UV178
ppm-1.D(jf120) III; chk-2(jf184[chk-2::ha]) V	This study	UV179
ppm-1.D(jf182[ppm-1.D(D274A)]) III; chk-2(jf184[chk-2::ha]) V	This study	UV180
ppm-1.D(jf181[ppm-1.D(tm8369+ D274A)]) III; chk-2(jf184[chk-2::ha]) V	This study	UV181
ppm-1.D(jf210[ha::ppm-1.D(tm8369)]) (LGIII); chk-2(jf185[chk-2::3×FLAG]) (LGV)	This study	UV269
ppm-1.D(jf208[HA::ppm-1.D(D274A)])	This study	UV270
ppm-1.D(jf207[HA::ppm-1.D(tm8369+D274A)])	This study	UV271
chk-2(jf184[chk-2::ha]) V	This study	UV182
ppm-1.D(jf183[ha::ppm-1.D]) III	This study	UV183
chk-2(jf185[chk-2::3×FLAG]) V; ppm-1.D(jf183 ha:: ppm-1.D]) III	This study	UV184
prom-1(ok1140)) unc-55(e402) I/ hT2[bli-4(e937) let-?(q782) qIs48](I;III)	This study	UV175
ppm-1.D(jf183[ha:: ppm-1.D]) III; prom-1(ok1140) unc-55(e402) /hT2[bli-4(e937) let-?(q782) qIs48](I;III)	This study	UV185
ppm-1.D(jf183[ha:: ppm-1.D]) III; prom-1(ok1140) unc-55(e402) /hT2[bli-4(e937) let-?(q782) qIs48](I;III); chk-2(jf185[chk-2::3×FLAG]) V	This study	UV238
spo-11(ok79)/nT1[unc-?(n754) let-? qIs50](IV;V).	(*62*)	AV106
ppm-1.D(tm8369) III; spo-11(ok79)/nT1[unc-?(n754) let-? qIs50](IV;V).	This study	UV186
ppm-1.D(jf120) III; spo-11(ok79)/nT1[unc-?(n754) let-? qIs50](IV;V).	This study	UV187
cep-1(gk138) I	(*63*)	TJ1
cep-1(gk138) I; ppm-1.D(tm8369)/qC1[dpy-19(e1259) glp-1(q339)] III	This study	UV188

cep-1(gk138) I; ppm-1.D(jf120)/qC1[dpy-19(e1259) glp-1(q339)] III	This study	UV189
ppm-1.D(jf183[ha::ppm-1.D]) III ; chk-2(me64) rol-9(sc148)/unc-51(e369) rol-9(sc148) V	This study	UV190
ppm-1.D(jf183[ha::ppm-1.D]) III; chkr-2(ok431) X	This study	UV237
ppm-1.D(jf183[ha::ppm-1.D]) III ; chk-2(me64) rol-9(sc148)/unc-51(e369) rol-9(sc148) V; chkr-2(ok431) X	This study	UV191
fog-2(oz40)	(*64*)	BS553
gld-2(q497) gld-1(q485)/hT2 [bli-4(e937) let-?(q782) qIs48] (I;III) I; ppm-1.D::AID::HA (kim61) III; ieSi38 [sun-1p::TIR1::mRuby::sun-1 3'UTR + Cbr-unc-119(+)] IV	This study	YKM393

Table S8.

Guide, repair template and genotyping primers used in this study in 5' to 3' orientation as DNA sequences.

Strain	crRNA (20 nt + NGG)	Repair template	Genotyping primer pair
prom-1::ha	GAGTCAAATTGAAGTTATGCCGG	For generation of the repair template the following pair of primers were used: Right arm forward: CGTCCCAGATTACGCTTAATTAGTGAGAAAATTATTATATCAGTATATAC Right arm reverse: GGAAACAGCTATGACCATGATTACGCCAAGCTTGCAAATCTCTCTCCCTTCCCCTC Left arm forward: ACGACGTTGTAAAACGACGGCCAGTGAATTCACTGGCGTACGAGTCAGGTG Left arm reverse: TAGTCTGGAACGTCGTATGGGTACAGTAGTTTCATTAATACTGGCATAAC	AGGAAAACTCGTGAGGTGCC GAGGGGACATTCACACGTAG
ppm-1.D(jf120)	TTCGCTAAAAACGAGTAAATCGG GACATTGTTCAGACTTAAAATGG	CATTTTCCAGCGATTTTATCGATTTTTTCGCCGTTTTTTTGCAGTTTTGAGTTGAAAAATCAAATCCCAGACATTGTTCAGACTTAAAATGGCAAAAGCTTCATCTCTATCGAAACTGGATGATGGAATTATTCGAGTTTCAGAAATTGCAGACGAAGAAGATGATGATGACGTCAC	CTCGTAAAATTTCAGTCTCGGGC CCCCTCATCATAGTGACGTCATC AATCGACAATAAATCCTCTCCGC
ppm-1.D(jf183[ha::ppm-1.D])	GACATTTTTCAGACCTAGAATGG	TTTTTTGCAGTTTTGAGTTGAAAAATCAAATCCCAGACATTTTTCAGACCTAGAATGTACCCATACGACGTCCCAGACTACGCCGGAGGAGGAGGAGGAGTGCAAACCAGTGAGCCGATGGCTCGAACACCCAT	TGATTTCAGTGGCTTTCAGACG TTCCCCAAATTGTATGGGTGTTCG
chk-2(jf184[chk-2::ha])	TGAAGTGGTGGGGACCCACGTGG	CCGATTTGACGACAAATTGCGGACTTTTGCGGCGGTGAAGTGGTGGGGACCCACGTGAAACGTTGTTCAGGCGTAGTCTGGGACGTCGTATGGGTATCCTCCTCCTCCTCCCATTTTTGCCTGAAAATAGGGTTTTTAAGGCTAAA	GACGCAATTACACCCGATTTGA TACACAAGCTGGACCTGTGA
ppm-1.D(jf182[ppm-1.D(CD)])	TTCCATCAGAAGCTAGTACGAGG	GCAGGAGTCCACCGGCTGACAGGAAATGACTTTTGTCTCGTACTCGCTTCAGCTGGAATGACAAATGTAATGACTGGTGATCAAGCAATATCA	CGCTGAAAACGCATAAAATTACGAA GGCAAACTTTCGAATAAATGCCAG

			Digest with *Pvu*II (edited is cut)
*chk-2(jf185[chk-2::**3×FLAG**])*	TGAAGTGGTGGGGACCCACGTGG	CCGATTTGACGACAAATTGCGGACTTTTGCGGCGGTGAAGTGGTGGGGACCCACGTGAAACGTTGTTCACTTGTCGTCGTCGTCCTTGTAGTCTCCTCCTCCTCCTCCCATTTTTGCCTGAAAATAGGGTTTTTAAGGCTAAA	GACGCAATTACACCCGATTTGA TACACAAGCTGGACCTGTGA
ppm-1.D(kim61[ppm-1.d::AID::HA])	ATATGAAAAAAATGGTTTGG	GACGATTTTTTGGATATATGAAAAAAATGGTTTGGGGAAAGGGAGGCTCAGGAATGCCTAAAGATCCAGCCAAACCTCCGGCCAAGGCACAAGTTGTGGGATGGCCACCGGTGAGATCATACCGGAAGAACGTGATGGTTTCCTGCCAAAAATCAAGCGGTGGCCCGGAGGCGGCGGCGTTCGTGAAGGGATCGTACCCATATGATGTGCCAGATTATGCCTAGTAATAAAGTTTTTTTTGAGATTTTTTAGACGTT	GAAGATGATGATGACGTCACTATG TTTCAGCCAATTTTCGCGTC

Table S9.

List of plasmids used in this study.

Plasmid description	Source	Identifier
Peft-3::cas9-SV40_NLS::tbb-2 3'UTR was a gift from John Calarco	(*65*)	Addgene plasmid # 46168
3xHA::loxP::Pmyo-2_GFP::Prpl-28_neoR::loxP; gift from Monica Colaiacovo	(*47*)	N/A
Co-injection marker Pmyo-2::mCherry::unc-54utr; gift from Erik Jorgensen	(*66*)	pCFJ90 Addgene plasmid # 19327
Co-injection marker pGH8 - pRAB-3::mCherry:: unc-54utr; gift from Erik Jorgensen	(*66*)	pGH8 Addgene plasmid # 19359
Peft-3::Cre	(*67*)	pDD104 Addgene plasmid # 47551
Homemade derivative of pBR322 (kanamycin resistance) GST-3C-CHK-2-(3×FLAG) (nematode CHK-2)	This study	N/A
Homemade derivative of pBR322 (kanamycin resistance) MBP-3C-PPM1D-His10 (nematode PPM-1.D)	This study	N/A
Homemade derivative of pBR322 (kanamycin resistance) MBP-3C-PPM1D (truncated)-His10 (nematode PPM-1.D)	This study	N/A
Homemade derivative of pBR322 (kanamycin resistance) 10xHIS-MBP-3C-NRDE2ΔN (human NRDE2)	This study	N/A
Homemade derivative of pDP134 (TRP1 auxotrophic marker, kanamycin resistance, 2 micron ori) ADH1_promoter-PPM-1.D-LexA-tADH1	This study	N/A
Homemade derivative of pDP134 (LEU2 auxotrophic marker, ampicillin resistance, 2 micron ori) ADH1_promoter-PROM-1-Gal4AD-HA-tADH1	This study	N/A

Table S10.

List of antibodies used in this study.

Antibodies	Source	Identifier
Primary antibodies for immuno-fluorescence		
Rat anti-HA (1:600)	Roche	Cat # 11867423001
Rabbit polyclonal anti-HA (1:1,000)	Sigma	Cat # H6908
Rabbit anti-WAPL-1 (1:2,000)	Novus	Cat # 49300002
Guinea pig polyclonal anti-HTP-3 (1:500)	(*23*)	N/A
Rabbit anti-SYP-1 (1:500)	Gift from Nicola Silva, Masaryk University, Czech Republic	N/A
Rat anti-REC-8 (1:100)	(*68*)	N/A
Guinea pig anti-SUN-1 (1:500)	(*10*)	N/A
Mouse anti-FLAG (1:1,000)	SIGMA	Cat # F3165
Rabbit anti-HIM-3 (1:750)	Novus	Cat # 53470002
Guinea pig anti-SUN-1(S8Pi) (1:750)	(*10*)	N/A
Mouse anti-CYE-1 (1:10)	(*69*)	N/A
Mouse anti-HA (1:500)	Thermo Fisher Scientific	Cat # 26183
Chicken anti-HIM-3 (1:500)	(*70*)	N/A
Rabbit anti-pHIM-8/ZIMs (1 ug/ml)	(*14*)	N/A
Secondary antibodies for immuno-fluorescence		
Goat anti-rabbit Alexa Fluor 568 (1:400)	Invitrogen	Cat # A-11036
Goat anti-guinea pig Alexa Fluor 488 (1:400)	Invitrogen	Cat # A-11073
Goat anti-mouse Alexa Fluor 594 (1:500)	Invitrogen	Cat # A-11032
Goat anti-rabbit 6 nm gold	Aurion	Cat # 800.011
Donkey anti-mouse Alexa Fluor 488 (1:200)	Invitrogen	Cat # A-21202
Donkey anti-rabbit Alexa Fluor 555 (1:200)	Invitrogen	Cat # A-31572
Donkey anti-chicken Alexa Fluor 647 (1:200)	Jackson ImmunoResearch	Cat# 703-605-155
Secondary antibodies for super resolution microscopy (STED)		
Anti-mouse Abberior STAR 635P (1:200)	Abberior	Cat # ST635P-1001
Anti-rabbit Abberior STAR 635P (1:200)	Abberior	Cat # ST635P-1007
Primary antibodies for Western blot		
Mouse monoclonal anti-HA (1:1,000)	Cell Signaling	Cat # 2367S
Rabbit polyclonal anti-histone H3 (1:100,000)	Abcam	Cat # ab1791
Secondary antibodies for Western blot		
Goat anti-rabbit HRP-conjugated (1:15,000)	Thermo Fisher	Cat # G21234
Goat anti-mouse HRP-conjugated (1:10,000)	Thermo Fisher	Cat # G21040

Table S11.

Primer pairs used for qRT-PCR.

Target RNA	**Primer forward**	**Primer reverse**
pmp-3	GCTGGAGTCACTCATCGTGTT	AGGACGATCAGTTTCAAGGCA
ppm-1.D(5' part)	CGACGTGTCCAGTGTAGAGTTT	AAATGCGCCATGTTTATGACGAA
ppm-1.D(3' part)	GTAGAACGCTGAACCAATCTCAAG	ATGATGTTAATGGAGAAGAGGACGAT

Table S12.

***P* values from Mann–Whitney tests comparing lethality rates in the different genotypes.** Significant *P* values (< 0.05) are highlighted in bold.

	Wild type	*prom-1(ok1140)*	*ppm-1.D(jf76)*	*ppm-1.D(jf76); prom-1(ok1140)*	*ppm-1.D(tm8369)*	*ppm-1.D(tm8369); prom-1(ok1140)*	*ppm-1.D(jf120)*	*ppm-1.D(jf120); prom-1(ok1140)*	*ppm-1.D(jf182)*	*ppm-1.D(jf182); prom-1(ok1140)*
Wild type	–	**< 0.0001**	**0.0003**	**< 0.0001**	**0.0039**	**< 0.0001**	**< 0.0001**	**< 0.0001**	**0.0011**	**< 0.0001**
prom-1(ok1140)	–	–	**< 0.0001**	**< 0.0001**	< 0.0001	**< 0.0001**	**< 0.0001**	**< 0.0001**	**< 0.0001**	**0.0004**
ppm-1.D(jf76)	–	–	–	**< 0.0001**	0.7655	**< 0.0001**	0.1545	**< 0.0001**	0.4890	**< 0.0001**
ppm-1.D(jf76); prom-1(ok1140)	–	–	–	–	**< 0.0001**	0.0522	**< 0.0001**	**0.0052**	**< 0.0001**	**< 0.0001**
ppm-1.D(tm8369)	–	–	–	–	–	**< 0.0001**	0.0627	**< 0.0001**	0.6706	**< 0.0001**
ppm-1.D(tm8369); prom-1(ok1140)	–	–	–	–	–	–	**< 0.0001**	**0.0015**	**< 0.0001**	**0.0003**
ppm-1.D(jf120)	–	–	–	–	–	–	–	**< 0.0001**	**0.0089**	**< 0.0001**
ppm-1.D(jf120); prom-1(ok1140)	–	–	–	–	–	–	–	–	**< 0.0001**	**< 0.0001**
ppm-1.D(jf182)	–	–	–	–	–	–	–	–	–	**< 0.0001**
ppm-1.D(jf182); prom-1(ok1140)	–	–	–	–	–	–	–	–	–	–

Table S13.

***P* values from Mann–Whitney tests comparing brood size in the different genotypes.** Significant *P* values (< 0.05) are highlighted in bold.

	Wild type	*prom-1(ok1140)*	*ppm-1.D(jf76)*	*ppm-1.D(jf76); prom-1(ok1140)*	*ppm-1.D(tm8369)*	*ppm-1.D(tm8369); prom-1(ok1140)*	*ppm-1.D(jf120)*	*ppm-1.D(jf120); prom-1(ok1140)*	*ppm-1.D(jf182)*	*ppm-1.D(jf182); prom-1(ok1140)*
Wild type	–	**0.0451**	**0.0493**	**0.0006**	0.3935	**0.0002**	0.0670	**< 0.0001**	0.4206	**< 0.0001**
prom-1(ok1140)	–	–	0.9116	**0.0100**	**0.0075**	**0.0010**	0.5607	**0.0001**	**0.0002**	**0.0010**
ppm-1.D(jf76)	–	–	–	0.2354	**0.0341**	**0.0104**	0.3509	**0.0002**	**0.0014**	**0.0155**
ppm-1.D(jf76); prom-1(ok1140)	–	–	–	–	**0.0001**	0.0639	**0.0029**	**0.0014**	**< 0.0001**	**0.0115**
ppm-1.D(tm8369)	–	–	–	–	–	**< 0.0001**	0.0749	**< 0.0001**	0.2394	**< 0.0001**
ppm-1.D(tm8369); prom-1(ok1140)	–	–	–	–	–	–	**0.0009**	0.5568	**< 0.0001**	0.6498
ppm-1.D(jf120)	–	–	–	–	–	–	–	**< 0.0001**	**0.0073**	**< 0.0001**
ppm-1.D(jf120); prom-1(ok1140)	–	–	–	–	–	–	–	–	**< 0.0001**	0.0782
ppm-1.D(jf182)	–	–	–	–	–	–	–	–	–	**< 0.0001**
ppm-1.D(jf182); prom-1(ok1140)	–	–	–	–	–	–	–	–	–	–

Table S14.

***P* values from Mann–Whitney tests comparing the percentage of males in hatched worms from the different genotypes.**

Significant *P* values (< 0.05) are highlighted in bold.

	Wild type	*prom-1(ok1140)*	*ppm-1.D(jf76)*	*ppm-1.D(jf76); prom-1(ok1140)*	*ppm-1.D(tm8369)*	*ppm-1.D(tm8369); prom-1(ok1140)*	*ppm-1.D(jf120)*	*ppm-1.D(jf120); prom-1(ok1140)*	*ppm-1.D(jf182)*	*ppm-1.D(jf182); prom-1(ok1140)*
Wild type	–	**0.0007**	> 0.9999	**0.0001**	0.4737	0.0867	0.0867	**0.0007**	> 0.9999	**0.0108**
prom-1(ok1140)	–	–	**0.0023**	**0.0347**	**0.0028**	**0.0070**	**0.0070**	**0.0257**	**0.0007**	0.0638
ppm-1.D(jf76)	–	–	–	**0.0001**	0.4737	0.0867	0.0867	**0.0007**	> 0.9999	**0.0108**
ppm-1.D(jf76); prom-1(ok1140)	–	–	–	–	**0.0002**	**0.0059**	**0.0006**	0.5281	**0.0001**	0.9703
ppm-1.D(tm8369)	–	–	–	–	–	0.1734	0.4334	**0.0013**	0.4737	**0.0251**
ppm-1.D(tm8369); prom-1(ok1140)	–	–	–	–	–	–	0.5756	**0.0113**	0.0867	0.0925
ppm-1.D(jf120)							–	**0.0036**	0.0867	0.0772
ppm-1.D(jf120); prom-1(ok1140)								–	**0.0007**	0.8925
ppm-1.D(jf182)									–	**0.0108**
ppm-1.D(jf182); prom-1(ok1140)										–

Table S15.

***P* values from Mann–Whitney tests comparing the number of DAPI bodies at diakinesis in the different genotypes.** Significant *P* values (< 0.05) are highlighted in bold.

	Wild type	*prom-1(ok1140)*	*ppm-1.D(jf76); prom-1(ok1140)*	*ppm-1.D(tm8369); prom-1(ok1140)*	*ppm-1.D(jf120); prom-1(ok1140)*	*ppm-1.D(jf182); prom-1(ok1140)*
Wild type	–	**< 0.0001**	0.7843	> 0.9999	> 0.9999	**< 0.0001**
prom-1(ok1140)	–	–	**< 0.0001**	**< 0.0001**	**< 0.0001**	0.1414
ppm-1.D(jf76); prom-1(ok1140)	–	–	–	> 0.9999	0.8706	**< 0.0001**
ppm-1.D(tm8369); prom-1(ok1140)	–	–	–	–	> 0.9999	**< 0.0001**
ppm-1.D(jf120); prom-1(ok1140)	–	–	–	–	–	**< 0.0001**
ppm-1.D(jf182); prom-1(ok1140)	–	–	–	–	–	–

REFERENCES AND NOTES

1. E. J. A. Hubbard, T. Schedl, Biology of the *Caenorhabditis elegans* germline stem cell system. *Genetics* **213**, 1145–1188 (2019).

2. A. Mohammad, K. vanden Broek, C. Wang, A. Daryabeigi, V. Jantsch, D. Hansen, T. Schedl, Initiation of meiotic development is controlled by three post-transcriptional pathways in *Caenorhabditis elegans*. *Genetics* **209**, 1197–1224 (2018).

3. D. Hansen, L. Wilson-Berry, T. Dang, T. Schedl, Control of the proliferation versus meiotic development decision in the *C. elegans* germline through regulation of GLD-1 protein accumulation. *Development* **131**, 93–104 (2004).

4. S. L. Crittenden, K. A. Leonhard, D. T. Byrd, J. Kimble, Cellular analyses of the mitotic region in the *Caenorhabditis elegans* adult germ line. *Mol. Biol. Cell* **17**, 3051–3061 (2006).

5. K. J. Hillers, V. Jantsch, E. Martinez-Perez, J. L. Yanowitz, Meiosis. *WormBook* **2017**, 1–43 (2017).

6. J. L. Gerton, R. S. Hawley, Homologous chromosome interactions in meiosis: Diversity amidst conservation. *Nat. Rev. Genet.* **6**, 477–487 (2005).

7. J. Link, V. Jantsch, Meiotic chromosomes in motion: A perspective from *Mus musculus* and *Caenorhabditis elegans*. *Chromosoma* **128**, 317–330 (2019).

8. V. Jantsch, L. Tang, P. Pasierbek, A. Penkner, S. Nayak, A. Baudrimont, T. Schedl, A. Gartner, J. Loidl, *Caenorhabditis elegans* prom-1 is required for meiotic prophase progression and homologous chromosome pairing. *Mol. Biol. Cell* **18**, 4911–4920 (2007).

9. A. J. MacQueen, A. M. Villeneuve, Nuclear reorganization and homologous chromosome pairing during meiotic prophase require *C. elegans* chk-2. *Genes Dev.* **15**, 1674–1687 (2001).

10. A. M. Penkner, A. Fridkin, J. Gloggnitzer, A. Baudrimont, T. Machacek, A. Woglar, E. Csaszar, P. Pasierbek, G. Ammerer, Y. Gruenbaum, V. Jantsch, Meiotic chromosome homology search involves modifications of the nuclear envelope protein Matefin/SUN-1. *Cell* **139**, 920–933 (2009).

11. A. Sato, B. Isaac, C. M. Phillips, R. Rillo, P. M. Carlton, D. J. Wynne, R. A. Kasad, A. F. Dernburg, Cytoskeletal forces span the nuclear envelope to coordinate meiotic chromosome pairing and synapsis. *Cell* **139**, 907–919 (2009).

12. J. Link, D. Paouneskou, M. Velkova, A. Daryabeigi, T. Laos, S. Labella, C. Barroso, S. P. Piñol, A. Montoya, H. Kramer, A. Woglar, A. Baudrimont, S. M. Markert, C. Stigloher, E. Martinez-Perez, A. Dammermann, M. Alsheimer, M. Zetka, V. Jantsch, Transient and partial nuclear lamina disruption promotes chromosome movement in early meiotic prophase. *Dev. Cell* **45**, 212–225.e7 (2018).

13. A. Woglar, V. Jantsch, Chromosome movement in meiosis I prophase of *Caenorhabditis elegans*. *Chromosoma* **123**, 15–24 (2014).

14. Y. Kim, N. Kostow, A. F. Dernburg, The chromosome axis mediates feedback control of CHK-2 to ensure crossover formation in *C. elegans*. *Dev. Cell* **35**, 247–261 (2015).

15. M. Castellano-Pozo, S. Pacheco, G. Sioutas, A. L. Jaso-Tamame, M. H. Dore, M. M. Karimi, E. Martinez-Perez, Surveillance of cohesin-supported chromosome structure controls meiotic progression. *Nat. Commun.* **11**, 4345 (2020).

16. E. L. Stamper, S. E. Rodenbusch, S. Rosu, J. Ahringer, A. M. Villeneuve, A. F. Dernburg, Identification of DSB-1, a protein required for initiation of meiotic recombination in *Caenorhabditis elegans*, illuminates a crossover assurance checkpoint. *PLoS genetics* **9**, e1003679 (2013).

17. S. Rosu, K. A. Zawadzki, E. L. Stamper, D. E. Libuda, A. L. Resse, A. F. Dernburg, A. M. Villeneuve, The *C. elegans* DSB-2 protein reveals a regulatory network that controls competence for meiotic DSB formation and promotes crossover assurance. *PLoS genetics* **9**, e1003674 (2013).

18. L. Tang, T. Machacek, Y. M. Mamnun, A. Penkner, J. Gloggnitzer, C. Wegrostek, R. Konrat, M. F. Jantsch, J. Loidl, V. Jantsch, Mutations in *Caenorhabditis elegans* him-19 show meiotic defects that worsen with age. *Mol. Biol. Cell* **21**, 885–896 (2010).

19. B. Simon-Kayser, C. Scoul, K. Renaudin, P. Jezequel, O. Bouchot, J. Rigaud, S. Bezieau, Molecular cloning and characterization of FBXO47, a novel gene containing an F-box domain, located in the

17q12 band deleted in papillary renal cell carcinoma. *Genes Chromosomes Cancer* **43**, 83–94 (2005).

20. S. Nayak, F. E. Santiago, H. Jin, D. Lin, T. Schedl, E. T. Kipreos, The *Caenorhabditis elegans* Skp1-related gene family: Diverse functions in cell proliferation, morphogenesis, and meiosis. *Curr. Biol.* **12**, 277–287 (2002).

21. X. Le Guezennec, D. V. Bulavin, WIP1 phosphatase at the crossroads of cancer and aging. *Trends Biochem. Sci.* **35**, 109–114 (2010).

22. O. Crawley, C. Barroso, S. Testori, N. Ferrandiz, N. Silva, M. Castellano-Pozo, A. L. Jaso-Tamame, E. Martinez-Perez, Cohesin-interacting protein WAPL-1 regulates meiotic chromosome structure and cohesion by antagonizing specific cohesin complexes. *eLife* **5**, e10851 (2016).

23. W. Goodyer, S. Kaitna, F. Couteau, J. D. Ward, S. J. Boulton, M. Zetka, HTP-3 links DSB formation with homolog pairing and crossing over during *C. elegans* meiosis. *Dev. Cell* **14**, 263–274 (2008).

24. A. J. MacQueen, M. P. Colaiacovo, K. McDonald, A. M. Villeneuve, Synapsis-dependent and -independent mechanisms stabilize homolog pairing during meiotic prophase in *C. elegans*. *Genes Dev* **16**, 2428–2442 (2002).

25. K. Schild-Prufert, T. T. Saito, S. Smolikov, Y. Gu, M. Hincapie, D. E. Hill, M. Vidal, K. M. Donald, M. P. Colaiácovo, Organization of the synaptonemal complex during meiosis in *Caenorhabditis elegans*. *Genetics* **189**, 411–421 (2011).

26. A. R. Goloudina, E. Y. Kochetkova, T. V. Pospelova, O. N. Demidov, Wip1 phosphatase: Between p53 and MAPK kinases pathways. *Oncotarget* **7**, 31563–31571 (2016).

27. H. Jaiswal, J. Benada, E. Müllers, K. Akopyan, K. Burdova, T. Koolmeister, T. Helleday, R. H. Medema, L. Macurek, A. Lindqvist, ATM/Wip1 activities at chromatin control Plk1 re-activation to determine G2 checkpoint duration. *EMBO J.* **36**, 2161–2176 (2017).

28. P. Bork, N. P. Brown, H. Hegyi, J. Schultz, The protein phosphatase 2C (PP2C) superfamily: Detection of bacterial homologues. *Protein Sci.* **5**, 1421–1425 (1996).

29. M. Fiscella, H. Zhang, S. Fan, K. Sakaguchi, S. Shen, W. E. Mercer, G. F. Vande Woude, P. M. O'Connor, E. Appella, Wip1, a novel human protein phosphatase that is induced in response to ionizing radiation in a p53-dependent manner. *Proc. Natl. Acad. Sci.* **94**, 6048–6053 (1997).

30. M. R. Dello Stritto, B. Bauer, P. Barraud, V. Jantsch, DNA topoisomerase 3 is required for efficient germ cell quality control. *J. Cell Biol.* **220**, e202012057 (2021).

31. I. A. Shaltiel, L. Krenning, W. Bruinsma, R. H. Medema, The same, only different—DNA damage checkpoints and their reversal throughout the cell cycle. *J. Cell Sci.* **128**, 607–620 (2015).

32. M. Takekawa, M. Adachi, A. Nakahata, I. Nakayama, F. Itoh, H. Tsukuda, Y. Taya, K. Imai, p53-inducible wip1 phosphatase mediates a negative feedback regulation of p38 MAPK-p53 signaling in response to UV radiation. *EMBO J.* **19**, 6517–6526 (2000).

33. P. M. Fox, V. E. Vought, M. Hanazawa, M.-H. Lee, E. M. Maine, T. Schedl, Cyclin E and CDK-2 regulate proliferative cell fate and cell cycle progression in the *C. elegans* germline. *Development* **138**, 2223–2234 (2011).

34. B. Biedermann, J. Wright, M. Senften, I. Kalchhauser, G. Sarathy, M.-H. Lee, R. Ciosk, Translational repression of cyclin E prevents precocious mitosis and embryonic gene activation during *C. elegans* meiosis. *Dev Cell* **17**, 355–364 (2009).

35. Z. Kocsisova, A. Mohammad, K. Kornfeld, T. Schedl, Cell cycle analysis in the *C. elegans* germline with the thymidine analog EdU. *J Vis Exp* **2018**, 58339 (2018).

36. M. C. Zetka, I. Kawasaki, S. Strome, F. Muller, Synapsis and chiasma formation in *Caenorhabditis elegans* require HIM-3, a meiotic chromosome core component that functions in chromosome segregation. *Genes Dev.* **13**, 2258–2270 (1999).

37. A. Alpi, P. Pasierbek, A. Gartner, J. Loidl, Genetic and cytological characterization of the recombination protein RAD-51 in *Caenorhabditis elegans*. *Chromosoma* **112**, 6–16 (2003).

38. M. P. Colaiacovo, A. J. MacQueen, E. Martinez-Perez, K. M. Donald, A. Adamo, A. L. Volpe, A. M. Villeneuve, Synaptonemal complex assembly in *C. elegans* is dispensable for loading strand-exchange proteins but critical for proper completion of recombination. *Dev Cell* **5**, 463–474 (2003).

39. T. L. Gumienny, E. Lambie, E. Hartwieg, H. R. Horvitz, M. O. Hengartner, Genetic control of programmed cell death in the *Caenorhabditis elegans* hermaphrodite germline. *Development* **126**, 1011–1022 (1999).

40. A. Gartner, S. Milstein, S. Ahmed, J. Hodgkin, M. O. Hengartner, A conserved checkpoint pathway mediates DNA damage—Induced apoptosis and cell cycle arrest in *C. elegans*. *Mol. Cell* **5**, 435–443 (2000).

41. A. Adamo, A. Woglar, N. Silva, A. Penkner, V. Jantsch, A. la Volpe, Transgene-mediated cosuppression and RNA interference enhance germ-line apoptosis in *Caenorhabditis elegans*. *Proc. Natl. Acad. Sci. U.S.A.* **109**, 3440–3445 (2012).

42. Y. Aubert, S. Egolf, B. C. Capell, The unexpected noncatalytic roles of histone modifiers in development and disease. *Trends Genetics* **35**, 645–657 (2019).

43. V. Reiterer, K. Pawłowski, G. Desrochers, A. Pause, H. J. Sharpe, H. Farhan, The dead phosphatases society: A review of the emerging roles of pseudophosphatases. *FEBS J.* **287**, 4198–4220 (2020).

44. S. Pechackova, K. Burdova, L. Macurek, WIP1 phosphatase as pharmacological target in cancer therapy. *J. Mol. Med.* **95**, 589–599 (2017).

45. S. Brenner, The genetics of *Caenorhabditis elegans*. *Genetics* **77**, 71–94 (1974).

46. A. Paix, A. Folkmann, D. Rasoloson, G. Seydoux, High efficiency, homology-directed genome editing in *Caenorhabditis elegans* using CRISPR-Cas9 ribonucleoprotein complexes. *Genetics* **201**, 47–54 (2015).

47. A. D. Norris, H. M. Kim, M. P. Colaiacovo, J. A. Calarco, Efficient genome editing in *Caenorhabditis elegans* with a toolkit of dual-marker selection cassettes. *Genetics* **201**, 449–458 (2015).

48. E. Martinez-Perez, A. M. Villeneuve, HTP-1-dependent constraints coordinate homolog pairing and synapsis and promote chiasma formation during *C. elegans* meiosis. *Genes Dev.* **19**, 2727–2743 (2005).

49. V. Jantsch, P. Pasierbek, M. M. Mueller, D. Schweizer, M. Jantsch, J. Loidl, Targeted gene knockout reveals a role in meiotic recombination for ZHP-3, a Zip3-related protein in *Caenorhabditis elegans*. *Mol. Cell. Biol.* **24**, 7998–8006 (2004).

50. R. S. Kamath, M. Martinez-Campos, P. Zipperlen, A. G. Fraser, J. Ahringer, Effectiveness of specific RNA-mediated interference through ingested double-stranded RNA in *Caenorhabditis elegans*. *Genome Biol* **2**, research0002.1 (2000).

51. Y. Zhang, D. Chen, M. A. Smith, B. Zhang, X. Pan, Selection of reliable reference genes in *Caenorhabditis elegans* for analysis of nanotoxicity. *PLOS ONE* **7**, e31849 (2012).

52. T. D. Schmittgen, K. J. Livak, Analyzing real-time PCR data by the comparative CT method. *Nat. Protoc.* **3**, 1101–1108 (2008).

53. N. Silva, N. Ferrandiz, C. Barroso, S. Tognetti, J. Lightfoot, O. Telecan, V. Encheva, P. Faull, S. Hanni, A. Furger, A. P. Snijders, C. Speck, E. Martinez-Perez, The fidelity of synaptonemal complex assembly is regulated by a signaling mechanism that controls early meiotic progression. *Dev. Cell* **31**, 503–511 (2014).

54. J. Chen, A. Mohammad, N. Pazdernik, H. Huang, B. Bowman, E. Tycksen, T. Schedl, GLP-1 Notch-LAG-1 CSL control of the germline stem cell fate is mediated by transcriptional targets lst-1 and sygl-1. *PLOS Genet.* **16**, e1008650 (2020).

55. C. Kraft, M. Kijanska, E. Kalie, E. Siergiejuk, S. S. Lee, G. Semplicio, I. Stoffel, A. Brezovich, M. Verma, I. Hansmann, G. Ammerer, K. Hofmann, S. Tooze, M. Peter, Binding of the Atg1/ULK1 kinase to the ubiquitin-like protein Atg8 regulates autophagy. *EMBO J.* **31**, 3691–3703 (2012).

56. J. Rappsilber, M. Mann, Y. Ishihama, Protocol for micro-purification, enrichment, pre-fractionation and storage of peptides for proteomics using StageTips. *Nat. Protoc.* **2**, 1896–1906 (2007).

57. M. Waas, M. Pereckas, R. A. Jones Lipinski, C. Ashwood, R. L. Gundry, SP2: Rapid and automatable contaminant removal from peptide samples for proteomic analyses. *J. Proteome Res.* **18**, 1644–1656 (2019).

58. J. Cox, M. Mann, MaxQuant enables high peptide identification rates, individualized p.p.b.-range mass accuracies and proteome-wide protein quantification. *Nat Biotechnol* **26**, 1367–1372 (2008).

59. R Core Team, R: A Language and Environment for Statistical Computing (2021).

60. M. E. Ritchie, B. Phipson, D. Wu, Y. Hu, C. W. Law, W. Shi, G. K. Smyth, *limma* powers differential expression analyses for RNA-sequencing and microarray studies. *Nucleic Acids Res.* **43**, e47 (2015).

61. K. T. Tokuyasu, A technique for ultracryotomy of cell suspensions and tissues. *J. Cell Biol.* **57**, 551–565 (1973).

62. A. F. Dernburg, K. McDonald, G. Moulder, R. Barstead, M. Dresser, A. M. Villeneuve, Meiotic recombination in *C. elegans* initiates by a conserved mechanism and is dispensable for homologous chromosome synapsis. *Cell* **94**, 387–398 (1998).

63. E. R. Hofmann, S. Milstein, S. J. Boulton, M. Ye, J. J. Hofmann, L. Stergiou, A. Gartner, M. Vidal, M. O. Hengartner, *Caenorhabditis elegans* HUS-1 is a DNA damage checkpoint protein required for genome stability and EGL-1-mediated apoptosis. *Curr. Biol.* **12**, 1908–1918 (2002).

64. R. Clifford, M. L. Lee, S. Nayak, M. Ohmachi, F. Giorgini, T. Schedl, FOG-2, a novel F-box containing protein, associates with the GLD-1 RNA binding protein and directs male sex determination in the *C. elegans* hermaphrodite germline. *Development* **127**, 5265–5276 (2000).

65. A. E. Friedland, Y. B. Tzur, K. M. Esvelt, M. P. Colaiácovo, G. M. Church, J. A. Calarco, Heritable genome editing in *C. elegans* via a CRISPR-Cas9 system. *Nat Methods* **10**, 741–743 (2013).

66. C. Frokjaer-Jensen, M Wayne Davis, C. E. Hopkins, B. J. Newman, J. M. Thummel, S.-P. Olesen, M. Grunnet, E. M. Jorgensen, Single-copy insertion of transgenes in *Caenorhabditis elegans*. *Nat. Genet.* **40**, 1375–1383 (2008).

67. D. J. Dickinson, J. D. Ward, D. J. Reiner, B. Goldstein, Engineering the *Caenorhabditis elegans* genome using Cas9-triggered homologous recombination. *Nat. Methods* **10**, 1028–1034 (2013).

68. P. Pasierbek, M. Jantsch, M. Melcher, A. Schleiffer, D. Schweizer, J. Loidl, A *Caenorhabditis elegans* cohesion protein with functions in meiotic chromosome pairing and disjunction. *Genes Dev.* **15**, 1349–1360 (2001).

69. T. M. Brodigan, J. Liu, M. Park, E. T. Kipreos, M. Krause, Cyclin E expression during development in *Caenorhabditis elegans*. *Dev. Biol.* **254**, 102–115 (2003).

70. M. E. Hurlock, I. Čavka, L. E. Kursel, J. Haversat, M. Wooten, Z. Nizami, R. Turniansky, P. Hoess, J. Ries, J. G. Gall, O. Rog, S. Köhler, Y. Kim, Identification of novel synaptonemal complex components in *C. elegans*. *J. Cell Biol.* **219**, e201910043 (2020).